

# CMOS CDBA-Based Inverse Filter Structure

Ram Bhagat, D. R. Bhaskar, Pragati Kumar

**Abstract:** This paper presents a voltage-mode (VM) tunable multifunction inverse filter configuration employing current differencing buffered amplifiers (CDBA). The presented structure utilizes two CDBAs, two/three capacitors and four/five resistors to realize inverse low pass filter (ILPF), inverse high pass filter (IHPF), inverse band pass filter (IBPF), and inverse band reject filter (IBRF) from the same circuit topology by suitable selection(s) of the branch admittances(s). PSPICE simulations have been performed with 0.18 $\mu$ m TSMC CMOS technology to validate the theory. Some sample experimental results have also been provided using off-the-shelf IC AD844 based CDBA.

**Keywords:** Analog Filters, Inverse Active Filters, Analog Signal Processing, CDBA

## I. INTRODUCTION

CDBA is an useful active building block (ABBs), which has been used widely in the field of analog signal processing and signal generation applications as it provides ideally zero input impedance at its input terminals and low output impedance (ideally zero at its output terminal).

Like filtering, inverse filtering is a frequency domain concept used in signal processing. It can be implemented in analog or in digital form. The transfer function of an analog active inverse filter is reciprocal to its conventional analog active filter. The inverse active filters are useful in removing the undesirable gain/phase alterations introduced in the signal while it is being processed by a system.

In past, several inverse active filters were reported using various active building blocks (ABBs) [1]-[11]. The notable features of these reported inverse active filters are shown in Table I. From Table I, it has been observed that there are limited number of CDBA-based inverse active filters [9]-[11]. In references [9] and [10], the intrinsic property of the CDBAs has not been fully utilized as n-terminals of both the CDBAs have been left open. In [11], conventional low pass filter, high pass filter, and band pass filter as well as ILPF, IHPF and IBPF have been reported from the same circuit topology.

This communication present a new multifunction inverse filter structure using two CDBAs, three/four resistors and two/three capacitors to realize second-order tunable ILPF, IHPF, IBPF and IBRF.

**Table I An overview of inverse active filter structures**

Ref.	No of ABBs	Resistors used	Capacitors used	Tunability
[1]	1 NULLOR	4	2	No
[2]	3 CFOA	4	2	No
[3]	3 CFOA	3-5	2	Yes
[4]	3 CFOA	3	3	No
[5]	3 CFOA	2-3	3-4	Yes
[6]	2 CFOA	4-6	2	No
[7]	2 OTRA	4	2/3	Yes
[8]	2 OTRA	4-5	3-4	Yes
[9]	2 CDBA	3	3	No
[10]	2 CDBA	2-4	2-4	No
[11]	2 CDBA	4	2	No
Proposed	2 CDBA	3/4	2/3	Yes

## II. PRESENTED CIRCUIT TOPOLOGY

The symbolic representation of CDBA is presented in Fig.1. The terminal voltage/current relationships are given in equation (1).

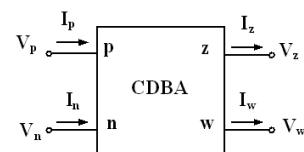


**Fig. 1 CDBA symbol**

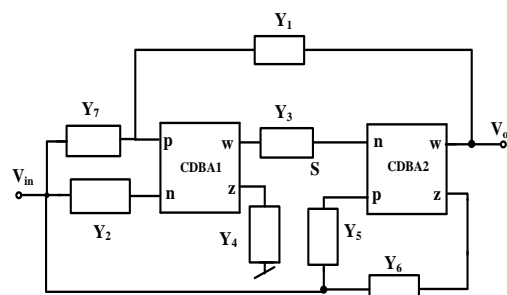


**Fig. 2 The presented inverse filter topology**

Revised Manuscript Received on January 5, 2020

\* Correspondence Author

**Ram Bhagat**, Electrical Engineering Department, Delhi Technological University, Delhi, India. Email: rambhagat@dtu.ac.in

**D. R. Bhaskar\***, Electronics and Communication Engineering Department, Delhi Technological University, Delhi, India. Email: drbhaskar@dtu.ac.in

**Pragati Kumar**, Electrical Engineering Department, Delhi Technological University, Delhi, India. Email: pragatikumar@dtu.ac.in

## CMOS CDBA-Based Inverse Filter Structure

$$V_p = 0 = V_n, I_z = (I_p - I_n), \text{ and } V_w = V_z \quad (1)$$

The circuit topology for the realization of ILPF, IHPF, IBPF and IBRF with seven branch admittances is shown in Fig.2

Assuming ideal CDBA, the ratio of output voltage to input voltage (TF) yields for the configuration shown in Fig. 2 can be obtained as:

$$TF = \frac{V_0}{V_{in}} = \frac{Y_4 Y_6 + Y_4 Y_5 + Y_7 Y_3}{Y_4 Y_6 + Y_1 Y_3} \text{ for } Y_2 = 2Y_7 \quad (2)$$

The proper choice(s) of admittance(s) yields ILPF, IHPF, IBPF and IBRF which has been shown in Table II. Table III shows the performance parameters  $\omega_0$ , BW and Q for the realized inverse active filters.

**Table II Realization of various inverse filter functions from the proposed configuration**

Type of filter realized	Choice of admittances							TF
	Y <sub>1</sub>	Y <sub>2</sub>	Y <sub>3</sub>	Y <sub>4</sub>	Y <sub>5</sub>	Y <sub>6</sub>	Y <sub>7</sub>	
ILPF	0	2C <sub>1</sub> s	$\frac{1}{R_3} + C_2s$	$\frac{1}{R_4}$	$\frac{1}{R_6}$	$\frac{1}{R_6}$	C <sub>1</sub> s	$\frac{1}{s^2 + \frac{1}{C_2R_3}s + \frac{2}{C_1C_2R_4R_6}}$
IHPF	0	$\frac{2}{R_2}$	$\frac{1}{R_3}$	C <sub>1</sub> s	$\frac{1}{R_5}$	C <sub>2</sub> s	$\frac{1}{R_2}$	$\frac{1}{s^2 + \frac{1}{C_2R_5}s + \frac{1}{C_1C_2R_2R_3}}$
IBPF	0	$\frac{2}{R_2}$	$\frac{1}{R_3}$	C <sub>1</sub> s	C <sub>2</sub> s	$\frac{1}{R_6}$	$\frac{1}{R_2}$	$\frac{s}{s^2 + \frac{1}{C_2R_6}s + \frac{1}{C_1C_2R_2R_3}}$
IBRF	$\frac{1}{R_2}$	$\frac{2}{R_2}$	$\frac{1}{R_3}$	C <sub>1</sub> s	$\frac{1}{R_5}$	C <sub>2</sub> s	$\frac{1}{R_2}$	$\frac{1}{s^2 + \frac{1}{C_1C_2R_2R_3}s + \frac{1}{C_2R_5}}$

**Table III Performance parameters of inverse filters of Table II**

Type of Filter realized	Cut-off frequency ( $\omega_0$ )	Bandwidth (BW)/Quality factor (Q)
ILPF	$\frac{1}{\sqrt{C_1C_2R_4R_6}}$	$Q = R_3 \sqrt{\frac{2C_2}{C_1R_4R_6}}$
IHPF	$\frac{1}{\sqrt{C_1C_2R_2R_3}}$	$Q = R_5 \sqrt{\frac{C_2}{C_1R_2R_3}}$
IBPF	$\frac{1}{\sqrt{C_1C_2R_2R_3}}$	$BW = \frac{1}{C_2R_6}$
IBRF	$\frac{1}{\sqrt{C_1C_2R_2R_3}}$	$BW = \frac{1}{C_2R_5}$

### III. SENSITIVITY ANALYSIS

Using the conventional definition of sensitivity of a function F(x) with respect to a parameter of interest x i.e.,

$$S_x^{F(x)} = \frac{x}{F(x)} \frac{\partial F(x)}{\partial x}, \text{ the sensitivities of } \omega_0, Q \text{ and BW of}$$

inverse active filters have been tabulated in Table IV. It may be observed from the Table IV that the sensitivities with respect to all passive components are low.

**Table IV Inverse filters sensitivity analysis**

Filter	Sensitivity
ILPF	$S_{R4}^{e0} = S_{R6}^{e0} = -\frac{1}{2}, S_{R3}^{e0} = 0, S_{C1}^{e0} = S_{C2}^{e0} = -\frac{1}{2}$ $S_{C1}^Q = S_{R4}^Q = S_{R6}^Q = -\frac{1}{2}, S_{C2}^Q = \frac{1}{2}, S_{R3}^Q = 1$
IHPF	$S_{R2}^{e0} = S_{R3}^{e0} = -\frac{1}{2}, S_{R5}^{e0} = 0, S_{C1}^{e0} = S_{C2}^{e0} = -\frac{1}{2}$ $S_{C1}^Q = S_{R3}^Q = S_{R2}^Q = -\frac{1}{2}, S_{C2}^Q = \frac{1}{2}, S_{R5}^Q = 1$
IBPF	$S_{R2}^{e0} = S_{R3}^{e0} = -\frac{1}{2}, S_{R6}^{e0} = 0, S_{C1}^{e0} = S_{C2}^{e0} = -\frac{1}{2}$ $S_{C2}^{BW} = S_{R6}^{BW} = -1, S_{C1}^{BW} = S_{R2}^{BW} = S_{R3}^{BW} = 0$
IBRF	$S_{R2}^{e0} = S_{R3}^{e0} = -\frac{1}{2}, S_{R5}^{e0} = 0, S_{C1}^{e0} = S_{C2}^{e0} = -\frac{1}{2}$ $S_{C2}^{BW} = S_{R5}^{BW} = -1, S_{C1}^{BW} = S_{R2}^{BW} = S_{R3}^{BW} = 0$

**IV. SIMULATION RESULTS**

The realized inverse filters have been simulated using CMOS CDBA [12] (which is reproduced here in Fig. 3) in PSPICE employing 0.18µm technology. The various aspect ratios of the MOSFETs have been taken from [12]. The bias voltages and bias currents used are ±2.5V and 40µA respectively. The proposed inverse active filters are designed for the ω<sub>0</sub> of 159 kHz and Q-factor of 0.707 by appropriate selection of the passive elements as:

**ILPF:** C<sub>1</sub> = C<sub>2</sub> = 100pF, R<sub>4</sub> = 1 kΩ, R<sub>5</sub> = R<sub>6</sub> = 14kΩ, R<sub>3</sub> = 7kΩ

**IHPF:** C<sub>1</sub> = C<sub>2</sub> = 100pF, R<sub>2</sub> = 5kΩ, R<sub>1</sub> = R<sub>3</sub> = R<sub>5</sub> = R<sub>7</sub> = 10kΩ

**IBPF:** C<sub>1</sub> = C<sub>2</sub> = 100pF, R<sub>2</sub> = 5kΩ, R<sub>1</sub> = R<sub>3</sub> = R<sub>5</sub> = R<sub>7</sub> = 10kΩ

**IBRF:** C<sub>1</sub> = C<sub>2</sub> = 100pF, R<sub>2</sub> = R<sub>3</sub> = R<sub>5</sub> = 10kΩ

Frequency (AC) responses of the inverse active filters are presented in Fig. 4, which establish the validity of the proposed circuit topology. The tunability for the cut-off frequency of proposed inverse active filters is shown in Fig. 5.

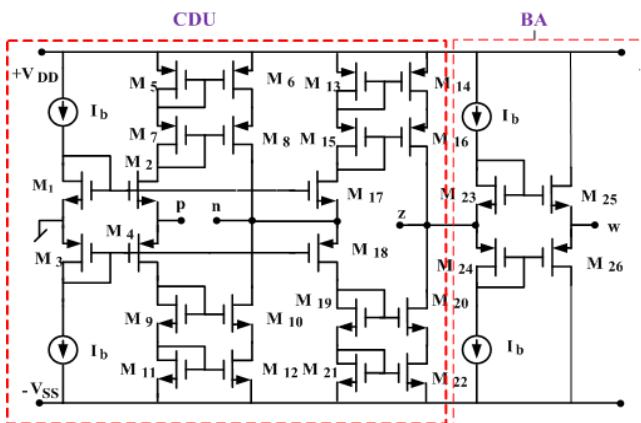
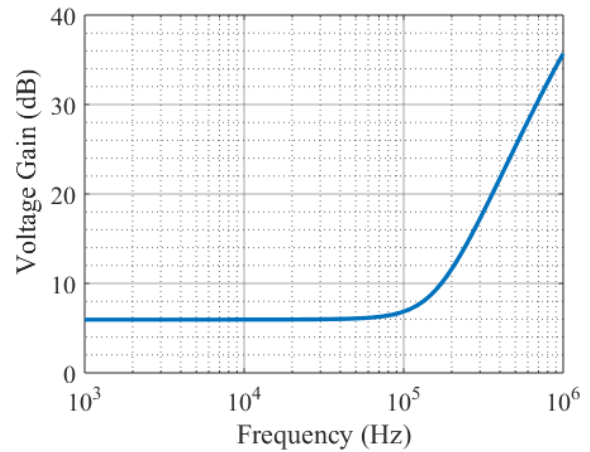
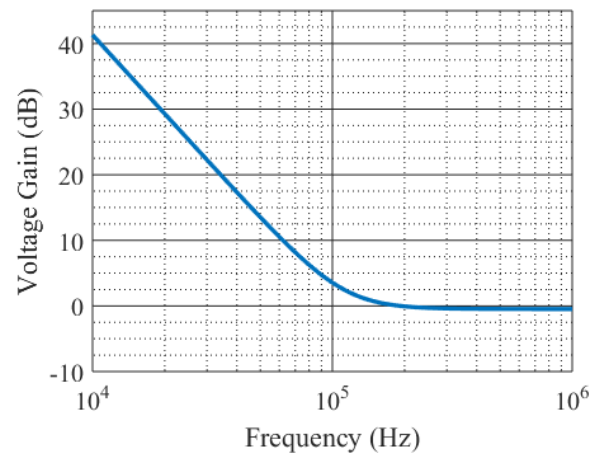


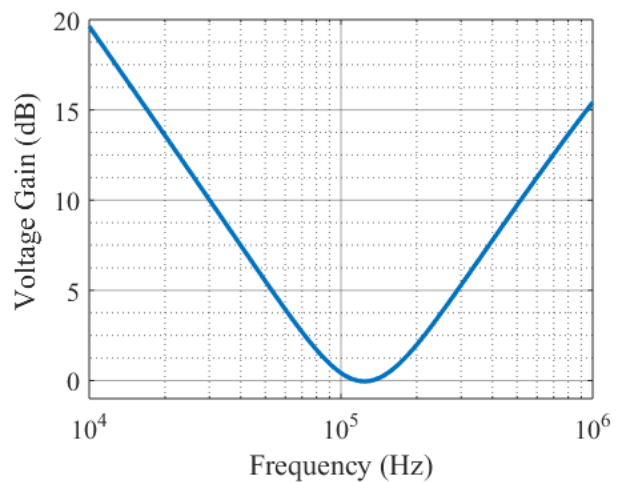
**Fig. 3. CDBA realization using CMOS [12]**



(a)



(b)



(c)

## CMOS CDBA-Based Inverse Filter Structure

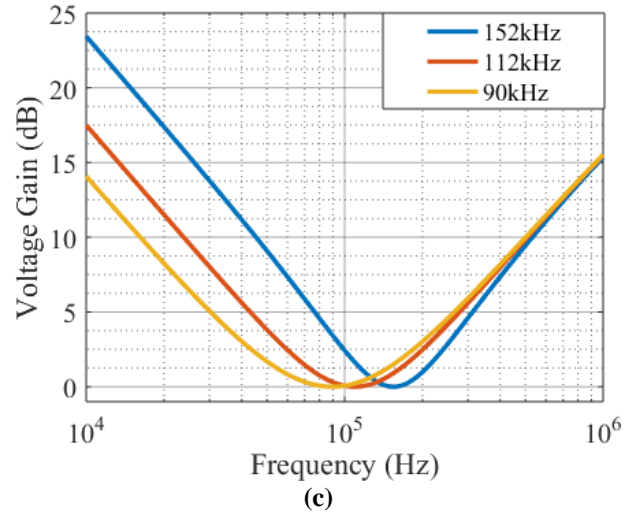
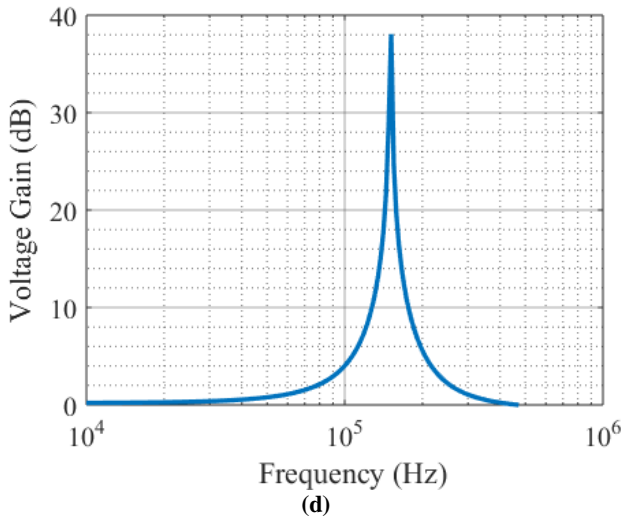


**Fig 4. AC responses of (a) ILPF (b) IHPF (c) IBPF and (d) IBRF**

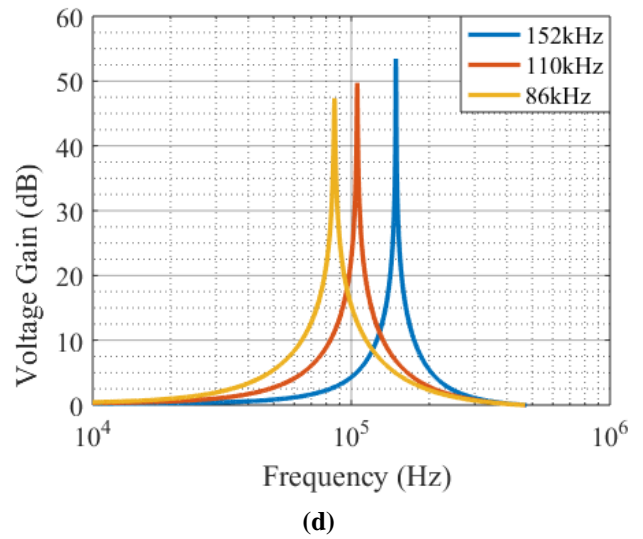
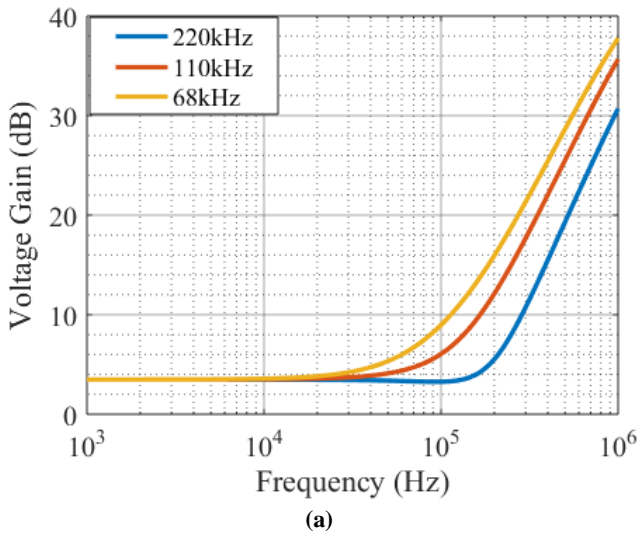


**Fig. 5 Tunability of cut-off frequency (a) ILPF (b) IHPF (c) IBPF and (d) IBRF**

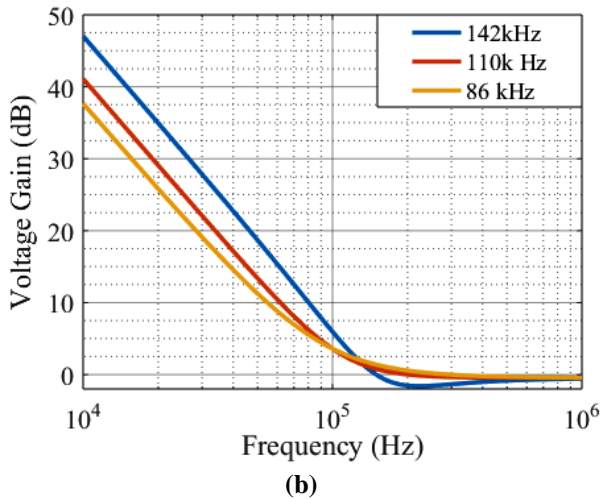
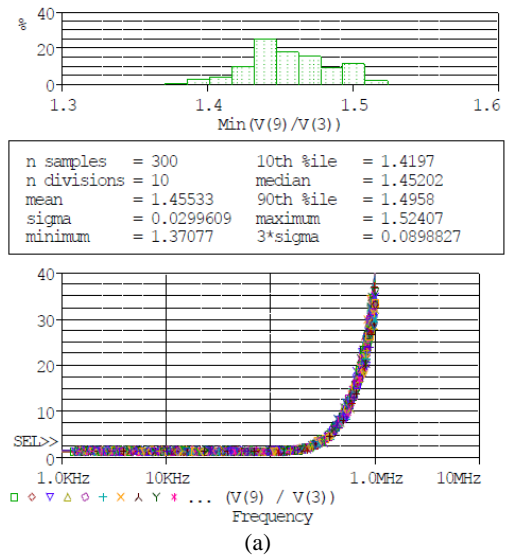
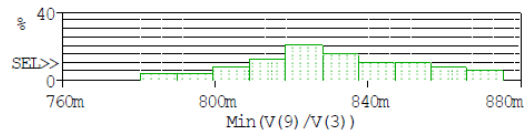
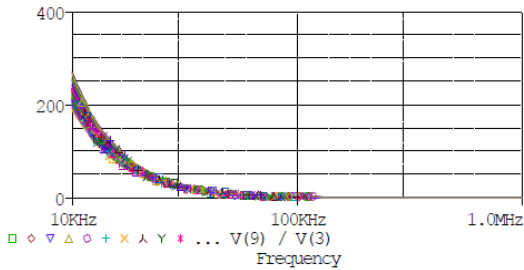


Fig. 6 presents variation in cut-off frequency and gain for the realized inverse active filters using Monte-Carlo simulations, for 5% variation in capacitor and resistor values.

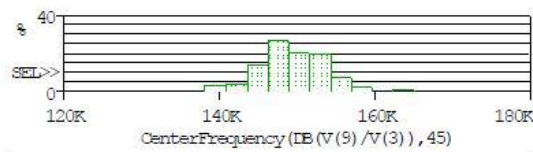




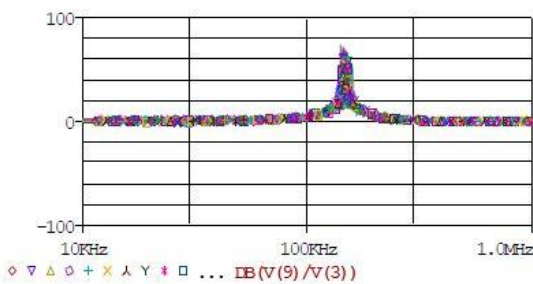
n samples = 100	10th %ile = 0.805473
n divisions = 10	median = 0.829164
mean = 0.830667	90th %ile = 0.860416
sigma = 0.0220868	maximum = 0.875493
minimum = 0.780407	3*sigma = 0.0662603



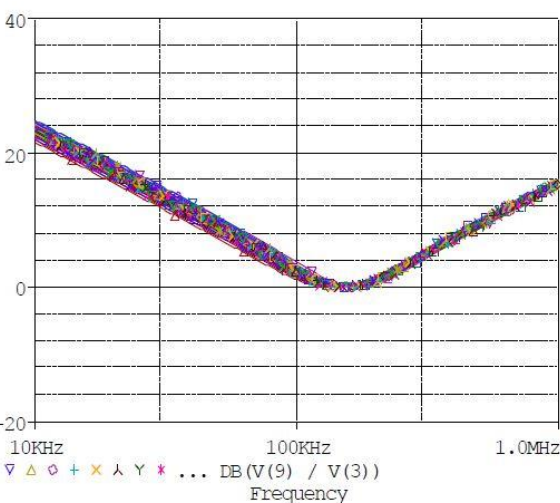
(b)



n samples = 100	10th %ile = 144323
n divisions = 10	median = 149382
mean = 149413	90th %ile = 154372
sigma = 4164.88	maximum = 165024
minimum = 138241	3*sigma = 12494.7



(c)



(d)

**Fig. 6 Histogram and AC responses of (a) ILPF (b) IHPF (c) IBPF and (d) IBRF using Monte-Carlo simulation for 5% variation in resistor and capacitor value**

Fig. 7 represents the implementation of CDBA using AD844 ff-the shelf IC. Some sample experimental results e.g. frequency response, transient response and frequency spectrum of IBRF are demonstrated in Fig 8 for 100 mV sinusoid input signal. The percentage total harmonic distortion (THD) obtained is 0.23 which is quite low.

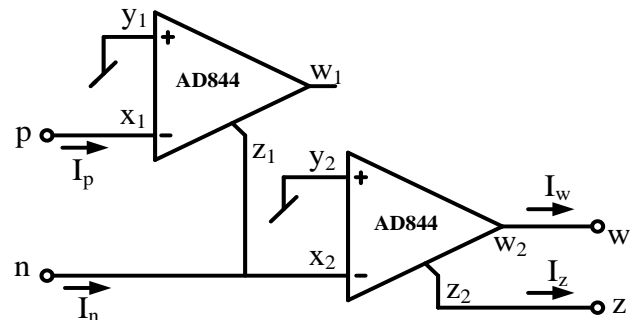
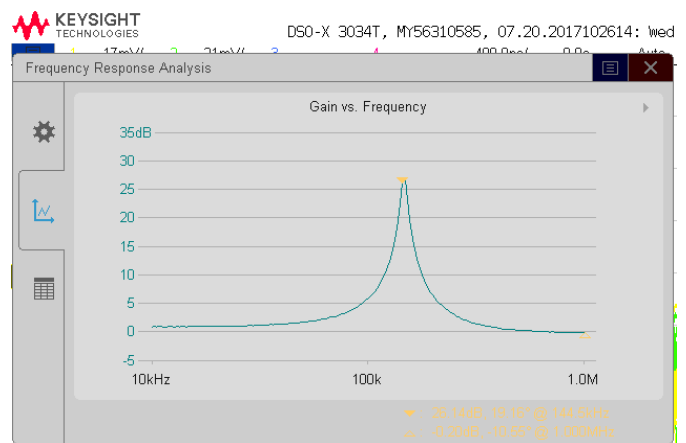
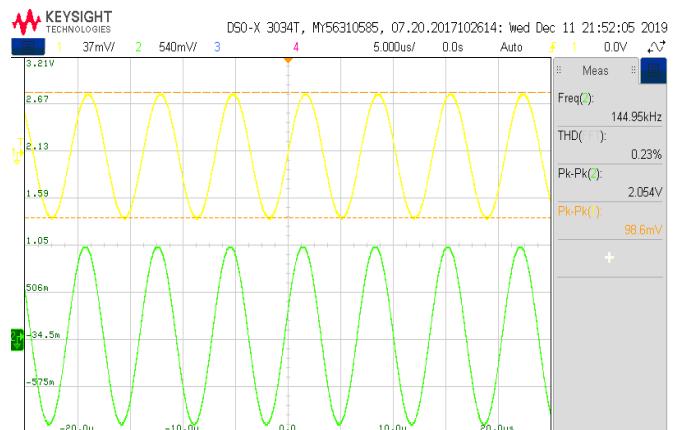


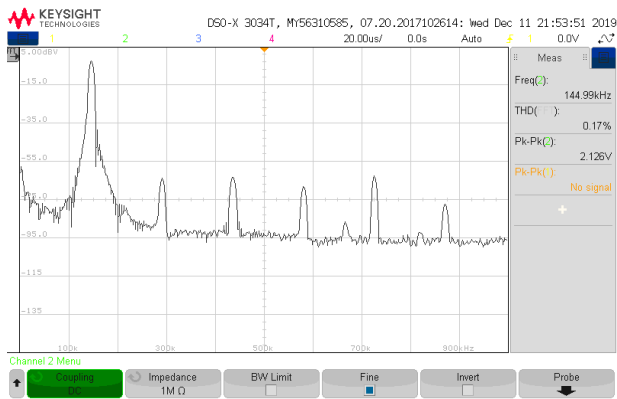
**Fig. 7 AD844 based implementation of CDBA**



**(a) Experimental AC response of IBRF**



**(b) Transient response of IBRF**



(c) Frequency spectrum of IBRF

Fig. 8 Experimental results of IBRF

## V. CONCLUDING REMARKS

A voltage-mode tunable inverse active filter circuit utilizing two CDBAs along with six/seven passive elements has been described. The presented configuration is capable of realising ILPF, IHPF, IBPF and IBRF from the same circuit configuration by proper selection(s) of admittance(s). The sensitivities of various performance parameters of all the inverse active filters have been calculated, from where it has been observed that the passive sensitivities are low. The robustness of the inverse filters has been checked through Monte-Carlo simulations. Some sample experimental results have also been incorporated to validate the workability of the presented structure.

## REFERENCES

1. Leuciuc, "Using nullors for realization of inverse transfer functions and characteristics", *Electro. Lett.*, 33(11) (1997), 949–951.
2. S. S. Gupta, D. R. Bhaskar, and R. Senani, A.K. Singh, "Inverse active filters employing CFOA", *Elect. Eng.* 1(2009), 23-26.
3. S. S. Gupta, D.R. Bhaskar, and R. Senani, "New analogue inverse filters realized with current feedback op-amp", *Int. j. of Electro.* 9(2011), 1103–1113.
4. H. Y. Wang, S.H. Chang, T.Y. Yang, and P.Y. Tsai, "A novel multifunction CFOA based inverse filter", *Circuits and Syst.* 2(2011), 14–17.
5. K. Garg, R. Bhagat, and B. Jaint, "A novel multifunction modified CFOA based inverse filter", In *Power Electronics (IICPE), IEEE 5th India International Conference.* (2012), 1-5.
6. V. N. Patil, and R. K. Sharma, "Novel inverse active filters employing CFOA", *Int. J. for Scientific Research & Develop.* 3(2015), 359–360.
7. A. K. Singh, A. Gupta, and R. Senani, "OTRA-based multi-function inverse filter configuration", *Adv. in Elect. and Electron. Eng.* 15(2018), 846-856.
8. A. Pradhan, and R. K. Sharma, "Generation of OTRA-Based Inverse All Pass and Inverse Band Reject Filters", *Proceedings of the National Acad. of Sci. India Section A: Physical Sciences*, 1-11 (2019) <https://doi.org/10.1007/s40010-019-00603-w>
9. A. R. Nasir, and S. N. Ahmad, "A new current mode multifunction inverse filter using CDBA", *Int. J. of Comp. Sc. and Info. Security*, 11(2013), 50-52.
10. R. Pandey, N. Pandey, and T. Negi, V. Garg, "CDBA based universal inverse filter", *ISRN Electronics*, (2013), 1-6.
11. R. Bhagat, D. R. Bhaskar, P. Kumar, "Multifunction Filter/Inverse Filter Configuration Employing CMOS CDBA", *International Journal of Recent Technology and Engineering*, ISSN: 2277-3878, Volume-8 Issue-4, 2019, 08(04), 8844-8853.
12. A.K. Singh, P. Kumar, "A novel fully differential current mode universal filter", In *Circuits and Systems (MWSCAS)*, 2014 IEEE 57th International Midwest Symposium, 579-582(2014).